Potential-density pairs for bent bars

D. Vogt[*]

P. S. Letelier[†]

Departamento de Matemática Aplicada-IMECC, Universidade
Estadual de Campinas 13083-970 Campinas, São Paulo, Brazil

November 15, 2018

Abstract

A method is presented to bend a thin massive line when the curvature is small. The procedure is applied to a homogeneous thin bar with two types of curvatures. One of them mimics a galactic bar with two spiral arms at its tips. It is showed that if the bending function is a linear combination of Legendre polynomials, then the bent potential is an exact solution of the Laplace equation. A transformation is applied on the thin bent bars to generate three-dimensional potential-density pairs without singularities. The potentials of the thin bent bars are also used to generate non-axisymmetric planar distributions of matter.

Key words: galaxies: kinematics and dynamics

1 Introduction

Bars are a common self-gravitating structure present in disc galaxies. About 50 per cent of such galaxies are stongly or weakly barred, including our Milky Way [1, 2]; see also the classification of galaxies by [3] and the fraction of barred galaxies discussed by [4, 5, 6]. Galactic bars are triaxial systems, and constructing analytical triaxial potential-density pairs is a difficult task. The only exact, self-consistent models of bars were constructed by Freeman [7], but they have some unrealistic features for barred systems. As alternatives, galactic bars have been approximately modelled as homogeneous ellipsoids [8, 9] or inhomogeneous prolate spheroids [10, 11, 12, 13]. In these works,

---

[*]e-mail: dvogt@ime.unicamp.br

[†]e-mail: letelier@ime.unicamp.br

the inhomogeneous bar has been represented by a Ferrers ellipsoid [14], which has a finite length and represents many features of galactic bars rather well. Long & Murali [15] found simple analytical potential density-pairs for prolate and triaxial bars that can all be expressed in terms of elementary functions. One of their model of bar was used in hydrodynamic simulations [16, 17, 18, 19, 20] to understand the response of a gaseous disc to the imposition of non-axisymmetric bar potentials.

Until recently, an unclear issue was the connection between bars and grand-design spirals. Many barred galaxies have spiral arms that appear to emerge from the tips of the bar (see, e.g., NGC 1300; [21], p. 525). However, [22] present evidences that the pattern speed of the spirals are much lower than the pattern speed of the bar, so the spiral cannot be driven directly by the bar. On the other hand, there are other observational evidences that bars and spiral arms are correlated [23, 24, 25, 26]. Salo et al. [27] recently investigated the relation between bar forcing and spiral density amplitudes for over 100 barred galaxies, and found that there exists a significant statistical correlation. Furthermore, hydrodynamics simulations of the response of a gaseous disc to the imposition of a non-axisymmetric bar [28, 29, 30, 31, 17, 32, 33, 34, 35, 19] have shown that the symmetric two-armed spirals in barred galaxies are driven by the gravitational torques of the bar.

The system bar+spiral arms may be viewed as a bar with bended ends, although we are not aware that such an interpretation has been proposed so far. It would be interesting to have simple, analytical models for such a gravitating system. In this work we propose a method to obtain potential-density pairs for thin and for 'softened' bent bars. In Section 2, we present a procedure to bend a thin massive line and to calculate its potential. The idea is to consider a slight curvature and expand the potential with respect to a small parameter. In Section 3 this formalism will be particularized to a thin bar with constant linear density. It will be shown that if the 'bending function' can be written in terms of Legendre polynomials, then the potential of the bent bar will be an *exact* solution of the Laplace equation. Two examples of deformed bars will be discussed. By using a suitable transformation, the thin bent bars are then 'softened' to generate three-dimensional potential-density pairs without singularities. In Section 4, we present non-axisymmetric potential density-pairs that represent planar distributions of matter constructed from the two potentials of bent bars discussed in Section 3. These planar potential-density pairs are found by using a method first proposed by Kuzmin [36]. The discussion of the results is left to Section 5.

2

2 Bent massive lines

In this section we present a procedure to bend a thin massive line. The curvature is supposed to be small, and the potential of the bent system will be obtained from an expansion of a small parameter. The undeformed massive line will be described by the parametric equations $x' = x_0(t)$, $y' = y_0(t)$, $z' = z_0(t)$, with $t \in [t_1, t_2]$. The gravitational potential $\Phi(\mathbf{r})$ of this line can be expressed as

$$\Phi = -G \int_{s_1}^{s_2} \frac{\lambda(s)\mathrm{d}s}{|\mathbf{r} - \mathbf{r}'|}, \tag{1}$$

where G is the gravitational constant, s is the arc length and $\lambda(s)$ is the linear density. In terms of the parameter t, equation (1) is rewritten as

$$\Phi = -G \int_{t_1}^{t_2} \frac{\lambda(t)|\dot{\mathbf{r}}'|\mathrm{d}t}{|\mathbf{r} - \mathbf{r}'|}, \tag{2}$$

where the dot represents derivative with respect to t.

We shall represent a slight curvature of the line as

$$\mathbf{r}' = \mathbf{r}_0(t) + \varepsilon \mathbf{r}_1(t), \tag{3}$$

where $\mathbf{r}_0(t)$ is the position of the undeformed line, ε is a small dimensionless parameter and the particular form of the curvature will be determined by the function $\mathbf{r}_1(t)$. We have, up to first order in ε,

$$|\dot{\mathbf{r}}'| = |\dot{\mathbf{r}}_0| + \varepsilon \frac{\dot{\mathbf{r}}_0 \cdot \dot{\mathbf{r}}_1}{|\dot{\mathbf{r}}_0|}, \tag{4}$$

$$\frac{1}{|\mathbf{r} - \mathbf{r}'|} = \frac{1}{|\mathbf{r} - \mathbf{r}_0|} + \varepsilon \frac{\mathbf{r}_1 \cdot (\mathbf{r} - \mathbf{r}_0)}{|\mathbf{r} - \mathbf{r}_0|^3}. \tag{5}$$

Thus, up to first order in ε, the potential (2) can be written as

$$\Phi = -G \int_{t_1}^{t_2} \frac{\lambda(t)|\dot{\mathbf{r}}_0|\mathrm{d}t}{|\mathbf{r} - \mathbf{r}_0|} - \varepsilon G \int_{t_1}^{t_2} \frac{\lambda(t)\dot{\mathbf{r}}_0 \cdot \dot{\mathbf{r}}_1 \mathrm{d}t}{|\dot{\mathbf{r}}_0||\mathbf{r} - \mathbf{r}_0|} - \varepsilon G \int_{t_1}^{t_2} \frac{\lambda(t)|\dot{\mathbf{r}}_0|\mathbf{r}_1 \cdot (\mathbf{r} - \mathbf{r}_0)\,\mathrm{d}t}{|\mathbf{r} - \mathbf{r}_0|^3}. \tag{6}$$

3 Bent bars

Now we consider the particular case of a bent bar with constant linear density. The undeformed bar located symmetrically on the z-axis with length $2a$

3

and linear density λ_0 will be parameterized by $\mathbf{r}_0 = (0, 0, t)$, with $t \in [-a, a]$. For simplicity, the 'bending function' $\mathbf{r}_1(t)$ will be chosen as $\mathbf{r}_1 = \big(0, f(t), 0\big)$. With these assumptions, the potential (6) reduces to

$$\Phi = \Phi_0 + \varepsilon \Phi_1, \tag{7}$$

where

$$\Phi_0 = -G\lambda_0 \int_{-a}^{a} \frac{\mathrm{d}t}{\sqrt{x^2 + y^2 + (z - t)^2}},$$

$$\Phi_1 = -G\lambda_0 \int_{-a}^{a} \frac{y f(t)\mathrm{d}t}{\left[x^2 + y^2 + (z - t)^2\right]^{3/2}}. \tag{8}$$

At this point it is convenient to relate the potentials (8) to an identity found by Letelier [37]:

$$Q_n(u) P_n(v) = \frac{1}{2} \int_{-a}^{a} \frac{P_n(t/a)\mathrm{d}t}{\sqrt{R^2 + (z - t)^2}}, \tag{9}$$

where P_n and Q_n are, respectively, the Legendre polynomials and the Legendre functions of the second kind, and (u, v) are the spheroidal coordinates related to the cylindrical coordinates (R, z) through

$$u = (R_1 + R_2)/(2a), \qquad v = (R_1 - R_2)/(2a), \tag{10}$$

$$R_1 = \sqrt{R^2 + (z + a)^2}, \qquad R_2 = \sqrt{R^2 + (z - a)^2}, \tag{11}$$

with $u \geq 1$ and $-1 \leq v \leq 1$. The physical interpretation of (9) is in terms of a bar with linear density proportional to a Legendre polynomial, whose potential corresponds to a multipole term that arises in a multipolar solution of the Einstein equations. The potential Φ_0 in (8) can thus be identified with

$$\Phi_0 = -2G\lambda_0 Q_0(u) P_0(v) = -2G\lambda_0 Q_0(u). \tag{12}$$

Furthermore, we note that Φ_1 can be rewritten as

$$\Phi_1 = -G\lambda_0 \int_{-a}^{a} \frac{y f(t)\mathrm{d}t}{\left[x^2 + y^2 + (z - t)^2\right]^{3/2}} = G\lambda_0 \frac{\partial}{\partial y} \int_{-a}^{a} \frac{f(t)\mathrm{d}t}{\sqrt{x^2 + y^2 + (z - t)^2}}. \tag{13}$$

If the function $f(t)$ can be expressed as a linear combination of Legendre polynomials, then the last integral in (13) may be directly integrated via the
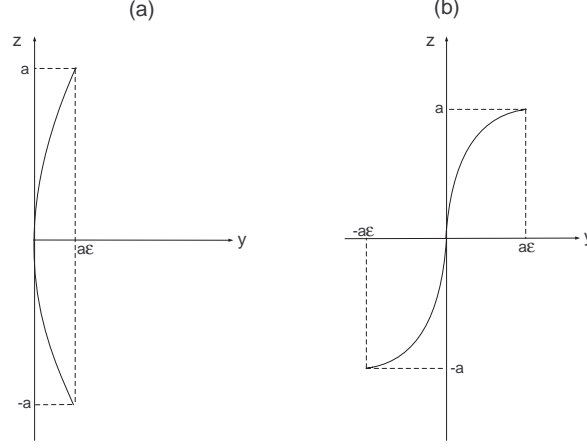
4

Figure 1: The shape of the bent bar for (a) the function $f(t) = t^2/a$, and (b) the function $f(t) = t^3/a^2$.

identity (9). This also shows that the potential Φ_1 will be then a solution of the Laplace equation, thus the potential (7) of the bent bar will also be an exact solution of the Laplace equation.

As examples, we will calculate the potential-density pairs for bars with two choices for the 'bending function' $\mathbf{r_1} = (0, f(t), 0)$. By (3), the parametric equations of the deformed bar are $x' = 0$, $y' = \varepsilon f(t)$ and $z' = t$, $t \in [-a, a]$, which may be rewritten as $y' = \varepsilon f(z')$, $-a \le z' \le a$. We shall take as first example $f(t) = t^2/a$ and then $f(t) = t^3/a^2$. The shape of the bent bar in each case is schematically depicted in Figs 1(a) and (b), respectively. The first shape does not represent necessarily a galactic bar, but we chose this bending function for its simplicity. The second shape mimics a bar with two spiral arms.

In terms of Legendre polynomials, we have

$$\frac{t^2}{a} = \frac{a}{3} P_0\left(\frac{t}{a}\right) + \frac{2a}{3} P_2\left(\frac{t}{a}\right), \tag{14}$$

$$\frac{t^3}{a^2} = \frac{3a}{5} P_1\left(\frac{t}{a}\right) + \frac{2a}{5} P_3\left(\frac{t}{a}\right). \tag{15}$$

It is then straightforward to calculate the potential (13) using the identity

(9), and we state the final result

$$\Phi_{(a)} = G\lambda_0 \ln\left(\frac{z-a+R_2}{z+a+R_1}\right) + \varepsilon\frac{G\lambda_0 y}{a}\left[\ln\left(\frac{z-a+R_2}{z+a+R_1}\right)\right.$$
$$\left. + \frac{a\left(x^2+y^2-z^2\right)(R_1+R_2) + z\left(x^2+y^2+z^2\right)(R_1-R_2)}{(x^2+y^2)\,R_1R_2}\right], \qquad (16)$$

$$\Phi_{(b)} = G\lambda_0 \ln\left(\frac{z-a+R_2}{z+a+R_1}\right) + \varepsilon\frac{G\lambda_0 y}{a^2\left(x^2+y^2\right)R_1R_2}$$
$$\times \left\{3z\left(x^2+y^2\right)R_1R_2\ln\left(\frac{z-a+R_2}{z+a+R_1}\right) + az\left(5x^2+5y^2-z^2\right)(R_1+R_2)\right.$$
$$\left. - (R_1-R_2)\left[a^2\left(x^2+y^2\right) + \left(x^2+y^2+z^2\right)\left(2x^2+2y^2-z^2\right)\right]\right\}, \qquad (17)$$

where $R_1 = \sqrt{x^2+y^2+(z+a)^2}$, $R_2 = \sqrt{x^2+y^2+(z-a)^2}$ and the subscripts (a) and (b) refer to the potentials calculated with the functions $f(t) = t^2/a$ and $f(t) = t^3/a^2$, respectively. The potential (16) remains invariant under the transformations $x \to -x$ or $z \to -z$, whereas the potential (17) remains invariant under the transformations $x \to -x$ or $y \to -y, z \to -z$.

3.1 Softened bent bars

The potentials (16)–(17) become singular along the bent thin bars. In order to get physically more realistic potentials it is convenient to 'soften' them. A simple way to achieve this is by means of a Plummer-like transformation [15]. In our examples we apply a transformation $x^2 + y^2 \to x^2 + y^2 + b^2$, where $b > 0$ is a 'softening' parameter. The corresponding three-dimensional mass density distribution is obtained from the Poisson equation in Cartesian coordinates, $\nabla^2\Phi(x, y, z) = 4\pi G\rho$. From the potential (16), after the transformation, we obtain the pair

$$\Phi_{(a)} = G\lambda_0 \ln\left(\frac{z-a+\mathcal{R}_2}{z+a+\mathcal{R}_1}\right) + \varepsilon\frac{G\lambda_0 y}{a}\left[\ln\left(\frac{z-a+\mathcal{R}_2}{z+a+\mathcal{R}_1}\right)\right.$$
$$\left. + \frac{a\left(x^2+y^2+b^2-z^2\right)(\mathcal{R}_1+\mathcal{R}_2) + z\left(x^2+y^2+b^2+z^2\right)(\mathcal{R}_1-\mathcal{R}_2)}{(x^2+y^2+b^2)\,\mathcal{R}_1\mathcal{R}_2}\right],$$
$$\qquad (18)$$

$$\rho_{(a)} = \rho_0 + \varepsilon\rho_1, \qquad (19)$$

6

where

$$\rho_0 = \frac{\lambda_0 b^2}{4\pi \left(x^2 + y^2 + b^2\right)^2 \mathcal{R}_1^3 \mathcal{R}_2^3} \left\{ \mathcal{R}_2^3 \left(z + a\right) \left[3\left(x^2 + y^2 + b^2\right) + 2\left(z + a\right)^2\right] \right.$$
$$\left. -\mathcal{R}_1^3 \left(z - a\right) \left[3\left(x^2 + y^2 + b^2\right) + 2\left(z - a\right)^2\right] \right\}, \tag{20}$$

$$\rho_1 = \frac{\lambda_0 y b^2}{4\pi a \left(x^2 + y^2 + b^2\right)^3 \mathcal{R}_1^5 \mathcal{R}_2^5} \left\{ 6z \left(x^2 + y^2 + b^2\right)^3 \left(\mathcal{R}_2^5 - \mathcal{R}_1^5\right) \right.$$
$$-\mathcal{R}_1^5 \left(z - a\right) \left[8z^2 \left(z - a\right)^4 + 2\left(z - a\right)^2 \left(x^2 + y^2 + b^2\right) \left(11z^2 - 2az + a^2\right) \right.$$
$$\left. +5\left(x^2 + y^2 + b^2\right)^2 \left(4z^2 - 2az + a^2\right)\right] + \mathcal{R}_2^5 \left(z + a\right) \left[8z^2 \left(z + a\right)^4 \right.$$
$$+2\left(z + a\right)^2 \left(x^2 + y^2 + b^2\right) \left(11z^2 + 2az + a^2\right)$$
$$\left. \left. +5\left(x^2 + y^2 + b^2\right)^2 \left(4z^2 + 2az + a^2\right)\right] \right\}, \tag{21}$$

where $\mathcal{R}_1 = \sqrt{x^2 + y^2 + b^2 + \left(z + a\right)^2}$, and $\mathcal{R}_2 = \sqrt{x^2 + y^2 + b^2 + \left(z - a\right)^2}$. Note that the first term of the potential (18) is the same as the potential of the prolate bar of [15] with the replacements $z \to x$ and $x^2 + y^2 \to y^2 + z^2 = R^2$.

Figs 2(a)–(c) display some curves of constant density of the dimensionless mass density $\bar{\rho}_{(a)} = \rho_{(a)}/(\lambda_0/a^2)$, equation (19), in the three orthogonal planes, with parameters $b/a = 0.25$ and $\varepsilon = 0.15$. The bending of the bar is apparent in the $y - z$ plane in Fig. 2(a). The density contours near the origin are bent in the same manner as the thin line of Fig. 1(a). There are two points of maximum that are shifted to the right of the z-axis, and two points of minimum appear on the opposite side. At these points the mass density may become negative as ε is increased; we found that for $b/a = 0.25$ the density is non-negative for $\varepsilon \lessapprox 0.16$. As the parameter b/a is increased for a fixed value of ε, the density contours become less elongated, the two points of minimum may disappear, and the two points of maximum move towards the origin. The contours in the $x - z$ plane preserve axial symmetry. Some level curves of the potential $\bar{\Phi}_{(a)} = \Phi_{(a)}/(G\lambda_0)$, equation (18), with parameters $b/a = 0.25$ and $\varepsilon = 0.15$, are displayed in Figs 3(a)–(c). In the $y - z$ plane the potential has only one minimum on $z = 0$ and $y = y_m$, which
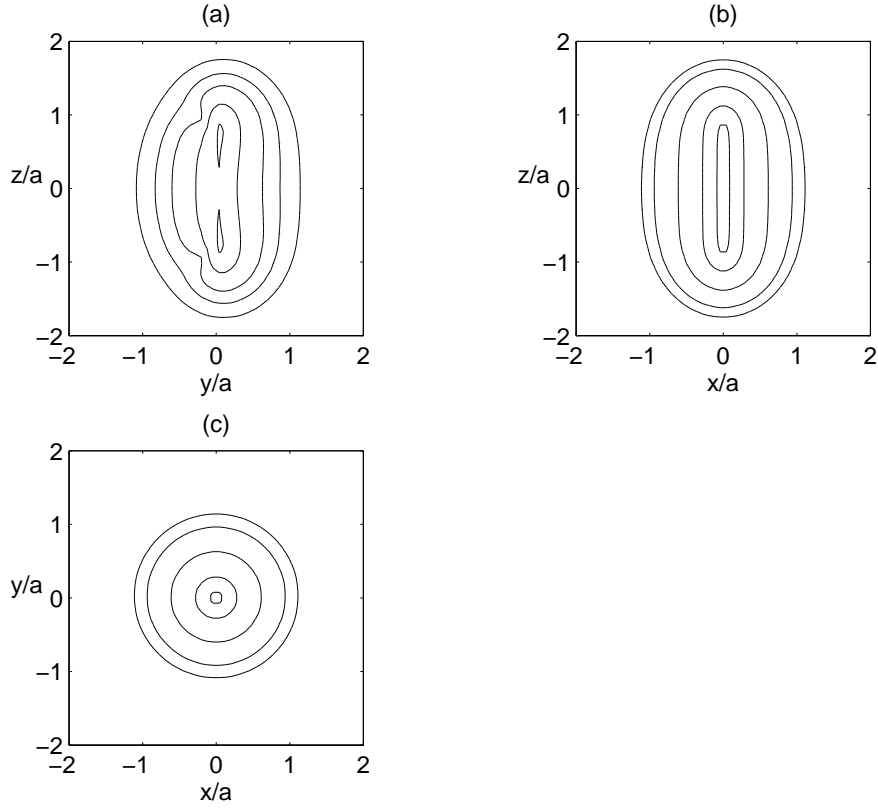
Figure 2: Isodensity contours of the mass density $\bar{\rho}_{(a)} = \rho_{(a)}/(\lambda_0/a^2)$, equation (19), in the three orthogonal coordinate planes. Parameters: $b/a = 0.25$, $\varepsilon = 0.15$.
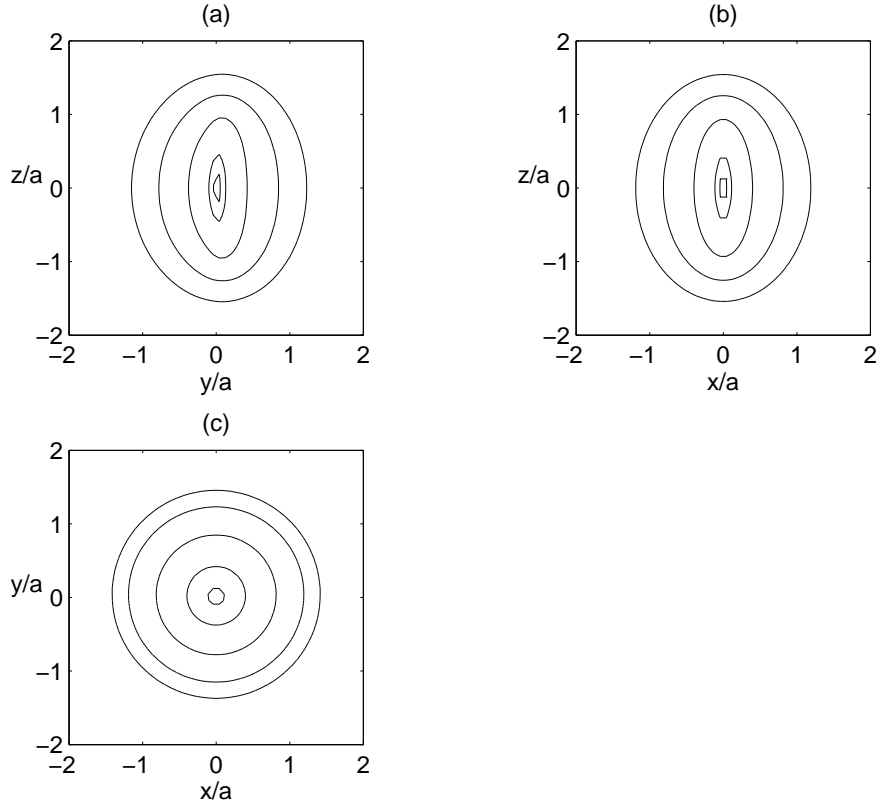
Figure 3: Isopotential contours of the potential $\bar{\Phi}_{(a)} = \Phi_{(a)}/(G\lambda_0)$, equation (18), in the three orthogonal coordinate planes. Parameters: $b/a = 0.25$, $\varepsilon = 0.15$.
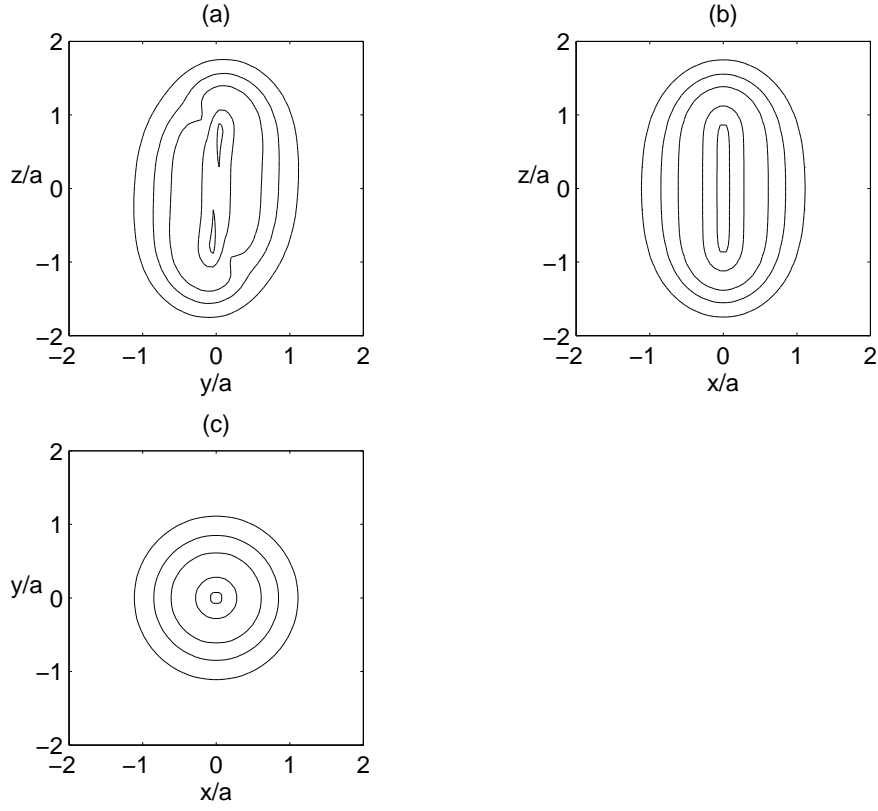
Figure 4: Isodensity contours of the mass density $\bar{\rho}_{(b)} = \rho_{(b)}/(\lambda_0/a^2)$, equation (24), in the three orthogonal coordinate planes. Parameters: $b/a = 0.25$, $\varepsilon = 0.15$.
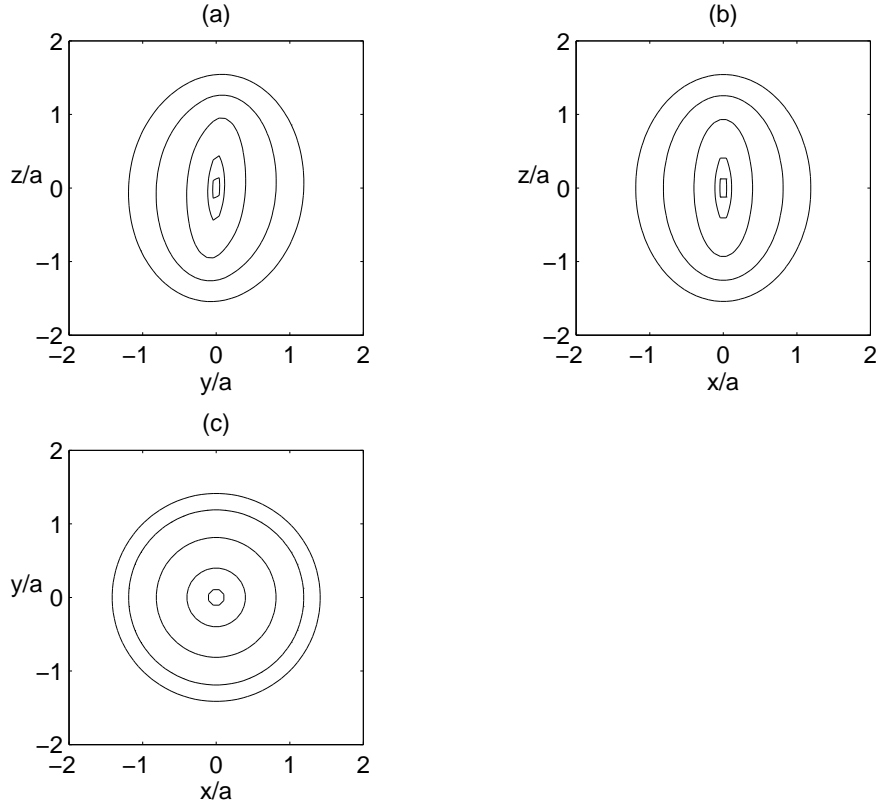
Figure 5: Isopotential contours of the potential $\bar{\bar{\Phi}}_{(b)} = \Phi_{(b)}/(G\lambda_0)$, equation (23), in the three orthogonal coordinate planes. Parameters: $b/a = 0.25$, $\varepsilon = 0.15$.

is the zero of

$$\frac{2ay_m}{(y_m^2 + b^2)\sqrt{y_m^2 + b^2 + a^2}} + \frac{\varepsilon}{a}\ln\left(\frac{\sqrt{y_m^2 + b^2 + a^2} - a}{\sqrt{y_m^2 + b^2 + a^2} + a}\right)$$

$$+ \frac{2\varepsilon\left[(y_m^2 + b^2)^2 + a^2\left(2y_m^2 + b^2\right)\right]}{(y_m^2 + b^2)(y_m^2 + b^2 + a^2)^{3/2}} = 0. \quad (22)$$

For the above-mentioned values of parameters the minimum occurs at $y_m/a \approx$ 0.011. The components of the force $\mathbf{F}_{(a)} = -\nabla\Phi_{(a)}$, corresponding to the potential (18), are listed in Appendix A.

Applying the same transformation on the potential (17) results in the potential-density pair:

$$\Phi_{(b)} = G\lambda_0 \ln\left(\frac{z - a + \mathcal{R}_2}{z + a + \mathcal{R}_1}\right) + \varepsilon\frac{G\lambda_0 y}{a^2\left(x^2 + y^2 + b^2\right)\mathcal{R}_1\mathcal{R}_2}$$

$$\times\left\{3z\left(x^2 + y^2 + b^2\right)\mathcal{R}_1\mathcal{R}_2\ln\left(\frac{z - a + \mathcal{R}_2}{z + a + \mathcal{R}_1}\right)\right.$$

$$+az\left(5x^2 + 5y^2 + 5b^2 - z^2\right)(\mathcal{R}_1 + \mathcal{R}_2) - (\mathcal{R}_1 - \mathcal{R}_2)\left[a^2\left(x^2 + y^2 + b^2\right)\right.$$

$$\left.\left. + \left(x^2 + y^2 + b^2 + z^2\right)\left(2x^2 + 2y^2 + 2b^2 - z^2\right)\right]\right\}, \quad (23)$$

$$\rho_{(b)} = \rho_0 + \varepsilon\rho_1, \quad (24)$$

where

$$\rho_1 = \frac{\lambda_0 y b^2}{4\pi a^2\left(x^2 + y^2 + b^2\right)^3\mathcal{R}_1^5\mathcal{R}_2^5}\left\{\mathcal{R}_2^5\left[8z^3\left(z + a\right)^5\right.\right.$$

$$+2z\left(z + a\right)^3\left(x^2 + y^2 + b^2\right)\left(13z^2 + 6az + 3a^2\right)$$

$$+15z\left(z + a\right)\left(x^2 + y^2 + b^2\right)^2\left(2z^2 + 2az + a^2\right)$$

$$\left. + \left(x^2 + y^2 + b^2\right)^3\left(14z^2 + 10az + 5a^2\right) + 2\left(x^2 + y^2 + b^2\right)^4\right]$$

$$-\mathcal{R}_1^5\left[8z^3\left(z - a\right)^5 + 2z\left(z - a\right)^3\left(x^2 + y^2 + b^2\right)\left(13z^2 - 6az + 3a^2\right)\right.$$

$$+15z\left(z - a\right)\left(x^2 + y^2 + b^2\right)^2\left(2z^2 - 2az + a^2\right)$$

$$\left.\left. + \left(x^2 + y^2 + b^2\right)^3\left(14z^2 - 10az + 5a^2\right) + 2\left(x^2 + y^2 + b^2\right)^4\right]\right\}, \quad (25)$$

and ρ_0 is given by (20). Some level curves in the three orthogonal planes of the mass density $\bar{\rho}_{(b)} = \rho_{(b)}/(\lambda_0/a^2)$, equation (24), are shown in Figs 4(a)–(c) with parameters $b/a = 0.25$ and $\varepsilon = 0.15$. The density contours near the origin are bent in the same manner as the thin line of Fig. 1(b). Two

points of maximum are present near the z-axis and two points of minimum are located antisymmetrically. The mass density may also become negative at these points with increasing values of ε, which can rise up to $\varepsilon \approx 0.18$ for $b/a = 0.25$. When the parameter b/a is increased with fixed ε, the point of minimum may disappear, the points of maximum approach the origin and the isodensity contours become more circular, in the same manner as in the previous case. Figs 5(a)–(c) display isopotential curves of the potential $\bar{\Phi}_{(b)} = \Phi_{(b)}/(G\lambda_0)$, equation (23), with parameters $b/a = 0.25$ and $\varepsilon = 0.15$. Here the minimum of potential is located at the origin. The components of the force $\mathbf{F}_{(b)} = -\nabla\Phi_{(b)}$ corresponding to the potential (23), are also given in Appendix A.

4   Non-axisymmetric thin distributions of matter

Non-axisymmetric thin distributions of matter are of interest since many galaxies exhibit asymmetries in their discs (see e.g. [38, 39] for observational evidences of asymmetries in disc galaxies). The potential of a thin bent bar may be used to generate non-axisymmetric thin distributions of matter. The procedure is similar to the one proposed by Kuzmin [36] to find the gravity field of an axisymmetric disc. A source of gravitational field is placed below a plane $z = 0$. Above the plane this gives a solution of the Laplace equation. The solution valid for $z \geq 0$ is then reflected with respect to $z = 0$ so as to give a symmetrical solution of the Laplace equation above and below the plane. This introduces a discontinuity in the normal derivative on $z = 0$, which by the Poisson equation results in a surface density. Kuzmin applied his procedure on a point mass. In general relativity, where the Schwarzschild solution in Weyl's metric is represented by a finite bar with constant density, Kuzmin's method has been used to construct 'generalized Schwarzschild' discs [40]. Some other examples of general relativistic discs generated by Kuzmin's method can be found in [41, 42, 43, 44].

We will place the thin bent bar along the x-axis and then displace it at a distance $c > 0$ below the plane $z = 0$, and make the reflection with respect to that plane. This is equivalent to first make the replacements $z \to x$ and $x \to z$ in the potentials (16)–(17), and further apply the transformation $z \to c + |z|$. By Poisson equation, the surface density σ on $z = 0$ is given by [21]

$$\sigma = \frac{1}{2\pi G} \left. \frac{\partial \Phi}{\partial z} \right|_{z=0}. \tag{26}$$

13

For the transformed potentials (16)–(17) we get, respectively,

$$\sigma_{(a)} = \frac{\lambda_0 c \left[(x+a)\,R_2 - (x-a)\,R_1\right]}{2\pi\,(y^2+c^2)\,R_1 R_2} - \varepsilon \frac{\lambda_0 c y}{2\pi a\,(y^2+c^2)^2\,R_1^3 R_2^3}$$
$$\times \left\{ R_1^3 \left[2x\,(x^2+y^2+c^2)^2 - a\,(y^2+c^2)\,(a^2-3ax+6x^2) \right.\right.$$
$$\left. -2ax^2\,(a^2-3ax+3x^2) \right] - R_2^3 \left[2x\,(x^2+y^2+c^2)^2 \right.$$
$$\left.\left. +a\,(y^2+c^2)\,(a^2+3ax+6x^2) + 2ax^2\,(a^2+3ax+3x^2) \right] \right\}, \qquad (27)$$

$$\sigma_{(b)} = \frac{\lambda_0 c \left[(x+a)\,R_2 - (x-a)\,R_1\right]}{2\pi\,(y^2+c^2)\,R_1 R_2} - \varepsilon \frac{\lambda_0 c y}{2\pi a^2\,(y^2+c^2)^2\,R_1^3 R_2^3}$$
$$\times \left\{ R_1^3 \left[2\,(x^2+y^2+c^2)^3 + 3a\,(y^2+c^2)^2\,(a-2x) \right.\right.$$
$$\left. -3ax\,(y^2+c^2)\,(a^2-3ax+4x^2) - 2ax^3\,(a^2-3ax+3x^2) \right]$$
$$-R_2^3 \left[2\,(x^2+y^2+c^2)^3 + 3a\,(y^2+c^2)^2\,(a+2x) \right.$$
$$\left.\left. +3ax\,(y^2+c^2)\,(a^2+3ax+4x^2) + 2ax^3\,(a^2+3ax+3x^2) \right] \right\}, \qquad (28)$$

where $R_1 = \sqrt{y^2+c^2+(x+a)^2}$ and $R_2 = \sqrt{y^2+c^2+(x-a)^2}$. Note that the first term in (27) and (28) is the surface density of a flat bar given by equation (11) of [15]. Although they obtained the result by convolution of a flat Miyamoto-Nagai disc (which is in fact a Kuzmin disc) with a needle density, our procedure gives the same result.

Some contours of the dimensionless surface density $\bar\sigma_{(a)} = \sigma_{(a)}/(\lambda_0/a)$ are shown in Fig. 6(a), for $c/a = 1$ and $\varepsilon = 2$, and in Fig. 6(b) for $c/a = 1$ and $\varepsilon = 0$. In both figures the level contours are plot for the same set of values. Figs 6(c) and (d) display contours of the potential $\bar\Phi_{(a)} = \Phi_{(a)}/(G\lambda_0)$ for the same parameters as in Figs 6(a) and (b), respectively. The isopotentials are also plot for the same set of values in both figures. Comparing the isodensity contours of the flat bent bar in Fig. 6(a) with the flat bar in Fig. 6(b), we note the asymetry with respect to the x-axis, with two points of minimum located symmetrically with respect to the y-axis. For $c/a = 1$, the surface density of the flat bent bar is everywhere non-negative provided $\varepsilon \lesssim 2.2$. The isopotential contours of the flat bent bar are shifted along the y-axis,
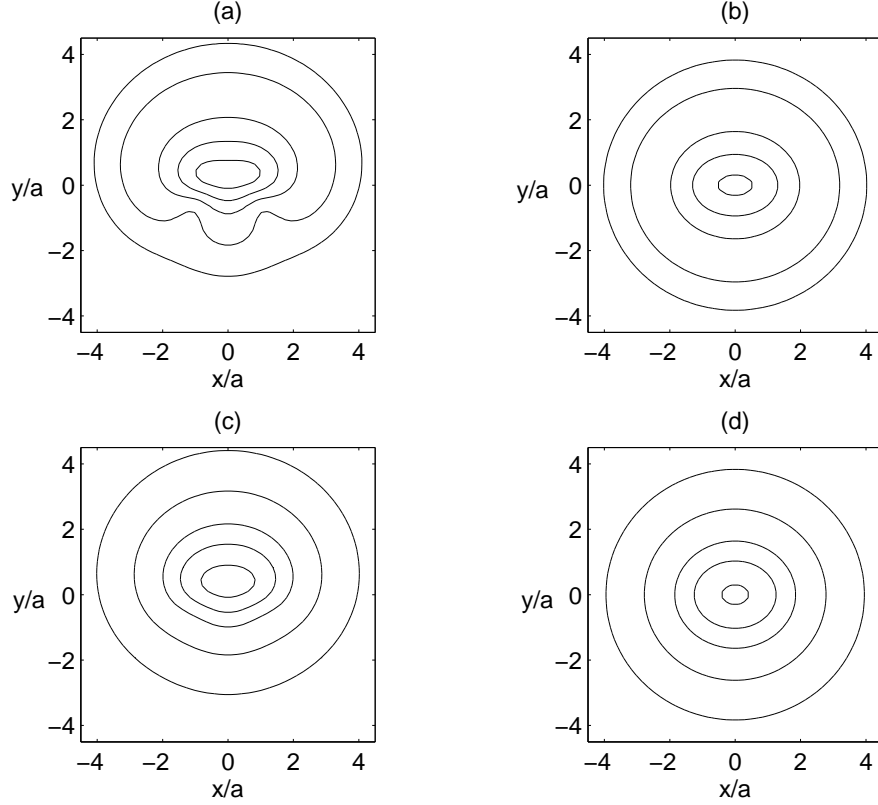
Figure 6: (a)–(b) Isodensity contours of the surface density $\bar{\sigma}_{(a)} = \sigma_{(a)}/(\lambda_0/a)$, equation (27). (a) Parameters: $c/a = 1$ and $\varepsilon = 2$. (b) Parameters: $c/a = 1$ and $\varepsilon = 0$. (c)–(d) Isopotential contours of the transformed potential $\bar{\Phi}_{(a)} = \Phi_{(a)}/(G\lambda_0)$ for the same parameters as in (a)–(b), respectively.
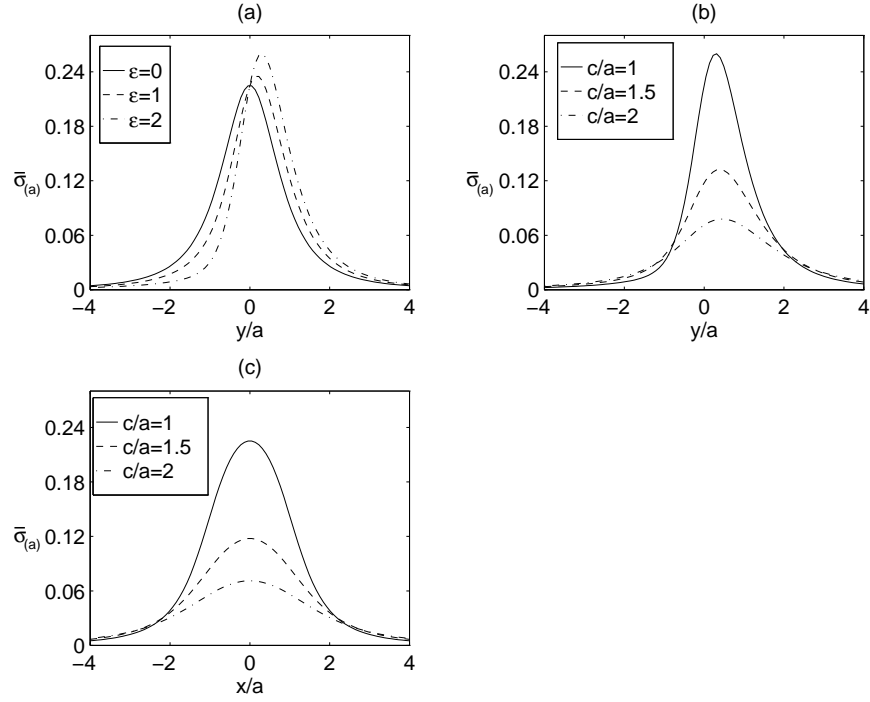
Figure 7: (a)–(b) Profiles of the surface density $\bar{\sigma}_{(b)} = \sigma_{(b)}/(\lambda_0/a)$, equation (27), along the y-axis, for different values of the parameters. (a) Parameters: $c/a = 1$ and $\varepsilon = 0$, 1 and 2. (b) Parameters: $\varepsilon = 2$ and $c/a = 1$, 1.5 and 2. (c) Profiles of the same surface density along the x-axis. Parameters: $c/a = 1$, 1.5 and 2.
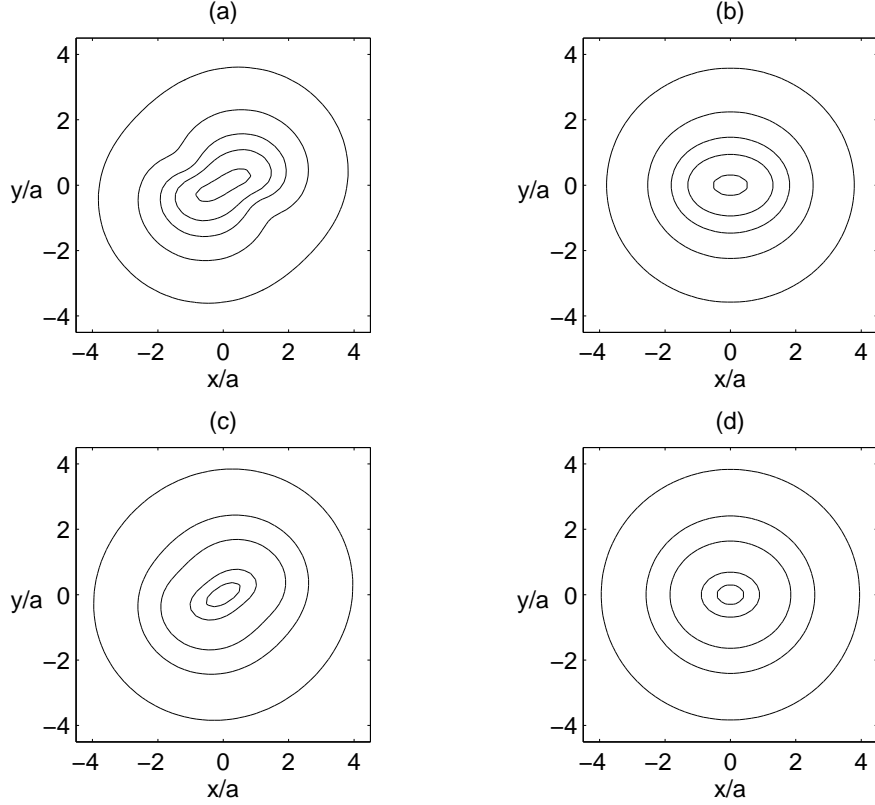
Figure 8: (a)–(b) Isodensity contours of the surface density $\bar{\sigma}_{(b)} = \sigma_{(b)}/(\lambda_0/a)$, equation (28). (a) Parameters: $c/a = 1$ and $\varepsilon = 2$. (b) Parameters: $c/a = 1$ and $\varepsilon = 0$. (c)–(d) Isopotential contours of the transformed potential $\bar{\Phi}_{(b)} = \Phi_{(b)}/(G\lambda_0)$ for the same parameters as in (a)–(b), respectively.

with a point of minimum at $x = 0$ and $y = y_m$, which is the zero of

$$\frac{2ay_m}{(y_m^2 + c^2)\sqrt{y_m^2 + c^2 + a^2}} + \frac{\varepsilon}{a}\ln\left(\frac{\sqrt{y_m^2 + c^2 + a^2} - a}{\sqrt{y_m^2 + c^2 + a^2} + a}\right)$$
$$+ \frac{2\varepsilon\left[\left(y_m^2 + c^2\right)^2 + a^2\left(2y_m^2 + c^2\right)\right]}{(y_m^2 + c^2)(y_m^2 + c^2 + a^2)^{3/2}} = 0, \quad (29)$$

an expression similar to (22). For the parameters $c/a = 1$ and $\varepsilon = 2$ we have $y_m/a \approx 0.376$.

In Figs 7(a)–(c) we display curves of the surface density $\bar{\sigma}_{(a)}$ along the y- and x-axes for some other values of the parameters c/a and ε. In Fig. 7(a) the parameter $c/a = 1$ is kept constant. With increasing values of ε, the asymmetry of the density profile with respect to $y = 0$ is enhanced. If we maintain $\varepsilon = 2$ constant, as in Fig. 7(b), the density distribution becomes somewhat less concentrated as the values of the parameter c/a increase. Fig. 7(c) shows curves of the surface density along the x-axis for the same values of c/a as in Fig. 7(b). From (27), it is seen that for $y = 0$ the profiles of the surface density of the flat bent bar and of the flat undeformed bar are the same, since the second term in (27) vanishes.

In Figs 8(a) and (b) we display some contours of the dimensionless surface density $\bar{\sigma}_{(b)} = \sigma_{(b)}/(\lambda_0/a)$, equation (28), for parameters $c/a = 1$ and $\varepsilon = 2$, and for $c/a = 1$ and $\varepsilon = 0$, respectively. In both figures the level contours are plot for the same set of values. Figs 8(c) and (d) display contours of the potential $\bar{\Phi}_{(b)} = \Phi_{(b)}/(G\lambda_0)$, for the same parameters as in Figs 8(a) and (b), respectively. The isopotentials are also plot for the same set of values in both figures. The surface density as well as the potential for this model of flat bent bar are asymmetric with respect to the x- and y-axes, in contrast to the potential-density pair of the flat undeformed bar. For the parameter $c/a = 1$, we find that the surface density of this model flat bent bar is everywhere non-negative provided $\varepsilon \lesssim 3.3$. The potential has a point of minimum at the origin. From (28) it is straightforward to see that the surface density profiles along the x- and y-axes are the same for the flat bent and for the flat undeformed bars.

In Appendix B, we list the components of the force $\mathbf{F}_{(a)} = -\nabla\Phi_{(a)}$, and of the force $\mathbf{F}_{(b)} = -\nabla\Phi_{(b)}$ on the plane $z = 0$, after applying the transformations $z \to x$ and $x \to z$, then $z \to c + |z|$, on the potentials (16)–(17).

18

5 Discussion

We presented a method to bend a thin massive line when the curvature is small. The potential of the bent system is obtained from an expansion with respect to a small parameter. The procedure was then applied to a homogeneous bar with two examples of 'bending functions'. We showed that if the 'bending function' can be expressed in terms of Legendre polynomials, then the potential of the bent bar is an exact solution of the Laplace equation. Potential-density pairs for 'softened' bent bars were constructed by using a Plummer-like transformation. The resulting mass density distributions are non-negative everywhere for restricted values of the deformation parameter ε. We also used the potentials of the bent thin bars to construct planar distributions of matter without axial symmetry. Furthermore, non-negative surface density distributions that are non-symmetric with respect to one or both x- and y-axes can be found for restricted values of the deformation parameter ε.

We would like to mention that the potential (6) of a bent massive line contains only terms originated from the expansion with respect to ε up to first order (dipole terms). In principle, higher order terms can be included, but we found that the explicit expressions, for instance the quadrupole terms, are very cumbersome. In particular, the quadrupolar terms can be explicitly found using the same algorithm employed for the dipolar terms.

A future work will be the study of orbits in the potentials of the 'softened' bent bars in an axisymmetric background with and without rotation and comparing the results with the works with undeformed bars, e.g. [10, 11, 12, 13].

Acknowledgments

References

[1] Sellwood J. A., Wilkinson A., 1993, Rep. Progress Phys., 56, 173

[2] Binney J., Merrifield M., 1998, Galactic Astronomy, Princeton Univ. Press, Princeton, NJ

[3] de Vaucouleurs G., 1963, ApJS, 8, 31

[4] Knapen J. H., 1999, in Beckman J. E., Mahoney T. J., eds, ASP Conf. Ser. Vol. 187, The Evolution of Galaxies on Cosmological Timescales. Astron. Soc. Pac., San Francisco, p. 72

[5] Eskridge P. B. et al., 2000, AJ, 119, 536

[6] Knapen J. H., Shlosman I., Peletier R. F., 2000, ApJ, 529, 93

[7] Freeman K. C., 1966, MNRAS, 134, 15

[8] Danby J. M. A., 1965, AJ, 70, 501

[9] Michalodimitrakis M., 1975, Ap&SS, 33, 421

[10] de Vaucouleurs G., Freeman K. C., 1972, Vistas Astron., 14, 163

[11] Athanassoula E., Bienayme O., Martinet L., Pfenniger D., 1983, A&A, 127, 349

[12] Papayannopoulos T., Petrou M., 1983, A&A, 119, 21

[13] Pfenniger D., 1984, A&A, 134, 373

[14] Ferrers N. M., 1877, Q. J. Pure Applied Math., 14, 1

[15] Long K., Murali C., 1992, ApJ, 397, 44

[16] Lee C. W., Lee H. M., Ann H. B., Kwon K. H., 1999, ApJ, 513, 242

[17] Ann H. B., Lee H. M., 2000, J. Korean Astron. Soc., 33, 1

[18] Ann H. B., Lee H. M., 2004, ApJ, 613, L105

[19] Ann H. B., Thakur P., 2005, ApJ, 620, 197

[20] Thakur P., Ann H. B., Jiang I.-G., 2009, ApJ, 693, 586

[21] Binney J., Tremaine S., 2008, Galactic Dynamics, 2nd edn. Princeton Univ. Press, Princeton, NJ

[22] Sellwood J. A., Sparke L. S., 1988, MNRAS, 231, 25p

[23] Elmegreen B. G., Elmegreen D. M., 1989, ApJ, 342, 677

[24] Block D. L., Puerari I., Knapen J. H., Elmegreen B. G., Buta R., Stedman S., Elmegreen D. M., 2001, A&A, 375, 761

[25] Block D. L., Buta R., Knapen J. H., Elmegreen D. M., Elmegreen B. G., Puerari I., 2004, AJ, 128, 183

[26] Buta R., Knapen J. H., Elmegreen B. G., Salo H., Laurikainen E., Elmegreen D. M., Puerari I., Block D. L., 2009, AJ, 137, 4487

[27] Salo H., Laurikainen E., Buta R., Knapen J. H., 2010, ApJ, 715, L56

[28] Athanassoula E., 1992, MNRAS, 259, 345

[29] Wada K., 1994, PASJ, 46, 165

[30] Englmaier P., Gerhard O. E., 1997, MNRAS, 287, 57

[31] Fukuda H., Wada K., Habe A., 1998, MNRAS, 295, 463

[32] Englmaier P., Shlosman I., 2000, ApJ, 528, 677

[33] Patsis P. A., Athanassoula E., 2000, A&A, 358, 45

[34] Maciejewski W., Teuben P. J., Sparke L. S., Stone J. M., 2002, MNRAS, 329, 502

[35] Maciejewski W., 2003, in Boily C. M., Patsis P., Portegies Zwart S., Spurzem R., Theis C., eds, Proc. JENAM 2002, Galactic and Stellar Dynamics. EDP Sciences, Les Ulis, p. 3

[36] Kuzmin G. G., 1956, AZh, 33, 27

[37] Letelier P. S., 1999, Classical Quantum Gravity, 16, 1207

[38] Baldwin J. E., Lynden Bell D., Sancisi R., 1980, MNRAS, 193, 313

[39] Richter O. -G., Sancisi R., 1994, A&A, 290, L9

[40] Bičák J., Lynden Bell D., Katz J., 1993, Phys. Rev. D, 47, 4334

[41] Bičák J., Lynden Bell D., Pichon C., 1993, MNRAS, 265, 126

[42] Lemos J. P. S., Letelier P. S., 1994, Phys. Rev. D, 49, 5135

[43] González G. A., Letelier P. S., 2000, Phys. Rev. D, 62, 064025

[44] Vogt D., Letelier P. S., 2003, Phys. Rev. D, 68, 084010

A Components of forces for bent bars

The components of the force $\mathbf{F}_{(a)}$ corresponding to the potential (18), are given by

$$F_{(a)x} = \frac{G\lambda_0 x \left[(z-a)\,\mathcal{R}_1 - (z+a)\,\mathcal{R}_2\right]}{(x^2+y^2+b^2)\,\mathcal{R}_1\mathcal{R}_2} + \varepsilon \frac{G\lambda_0 xy}{a\,(x^2+y^2+b^2)^2\,\mathcal{R}_1^3\mathcal{R}_2^3}$$

$$\times \left\{\mathcal{R}_1^3 \left[2z\left(x^2+y^2+b^2+z^2\right)^2 - a\left(x^2+y^2+b^2\right)\left(a^2-3az+6z^2\right)\right.\right.$$

$$\left.-2az^2\left(a^2-3az+3z^2\right)\right] - \mathcal{R}_2^3 \left[2z\left(x^2+y^2+b^2+z^2\right)^2\right.$$

$$\left.\left.+a\left(x^2+y^2+b^2\right)\left(a^2+3az+6z^2\right) + 2az^2\left(a^2+3az+3z^2\right)\right]\right\}, \qquad (30)$$

$$F_{(a)y} = \frac{G\lambda_0 y \left[(z-a)\,\mathcal{R}_1 - (z+a)\,\mathcal{R}_2\right]}{(x^2+y^2+b^2)\,\mathcal{R}_1\mathcal{R}_2} - \varepsilon \frac{G\lambda_0}{a}\ln\left(\frac{z-a+\mathcal{R}_2}{z+a+\mathcal{R}_1}\right)$$

$$+\varepsilon \frac{G\lambda_0}{a\,(x^2+y^2+b^2)^2\,\mathcal{R}_1^3\mathcal{R}_2^3}\left\{\mathcal{R}_1^3\left[z\left(x^2+y^2+b^2+z^2\right)^2\left(y^2-x^2-b^2\right)\right.\right.$$

$$\left.-a\left(x^2+y^2+b^2+z^2\right)\left[3z^2\left(y^2-x^2-b^2\right) + \left(x^2+y^2+b^2\right)^2\right]\right.$$

$$\left.-a^2\left(x^2+y^2+b^2\right)\left[a\left(x^2+2y^2+b^2\right) - z\left(x^2+4y^2+b^2\right)\right]\right.$$

$$\left.-a^2z^2\left(y^2-x^2-b^2\right)(a-3z)\right] - \mathcal{R}_2^3\left[z\left(x^2+y^2+b^2+z^2\right)^2\left(y^2-x^2-b^2\right)\right.$$

$$\left.+a\left(x^2+y^2+b^2+z^2\right)\left[3z^2\left(y^2-x^2-b^2\right) + \left(x^2+y^2+b^2\right)^2\right]\right.$$

$$\left.+a^2\left(x^2+y^2+b^2\right)\left[a\left(x^2+2y^2+b^2\right) + z\left(x^2+4y^2+b^2\right)\right]\right.$$

$$\left.\left.+a^2z^2\left(y^2-x^2-b^2\right)(a+3z)\right]\right\}, \qquad (31)$$

$$F_{(a)z} = \frac{G\lambda_0\,(\mathcal{R}_2-\mathcal{R}_1)}{\mathcal{R}_1\mathcal{R}_2} + \varepsilon \frac{G\lambda_0 y}{a\,(x^2+y^2+b^2)\,\mathcal{R}_1^3\mathcal{R}_2^3}\left\{\mathcal{R}_2^3\left[2\left(x^2+y^2+b^2+z^2\right)^2\right.\right.$$

$$\left.+3a\left(x^2+y^2+b^2\right)(a+2z) + 2az\left(a^2+3az+3z^2\right)\right]$$

$$-\mathcal{R}_1^3\left[2\left(x^2+y^2+b^2+z^2\right)^2 + 3a\left(x^2+y^2+b^2\right)(a-2z)\right.$$

$$\left.\left.-2az\left(a^2-3az+3z^2\right)\right]\right\}. \qquad (32)$$

The components of the force $\mathbf{F}_{(b)}$ corresponding to the potential (23),

22

are given by

$$F_{(b)x} = \frac{G\lambda_0 x\left[(z-a)\,\mathcal{R}_1 - (z+a)\,\mathcal{R}_2\right]}{(x^2+y^2+b^2)\,\mathcal{R}_1\mathcal{R}_2} + \varepsilon\frac{G\lambda_0 xy}{a^2\,(x^2+y^2+b^2)^2\,\mathcal{R}_1^3\mathcal{R}_2^3}$$

$$\left\{\mathcal{R}_1^3\left[2\left(x^2+y^2+b^2+z^2\right)^3 + 3a\left(x^2+y^2+b^2\right)^2(a-2z)\right.\right.$$

$$\left.-3az\left(x^2+y^2+b^2\right)\left(a^2-3az+4z^2\right) - 2az^3\left(a^2-3az+3z^2\right)\right]$$

$$-\mathcal{R}_2^3\left[2\left(x^2+y^2+b^2+z^2\right)^3 + 3a\left(x^2+y^2+b^2\right)^2(a+2z)\right.$$

$$\left.\left.+3az\left(x^2+y^2+b^2\right)\left(a^2+3az+4z^2\right) + 2az^3\left(a^2+3az+3z^2\right)\right]\right\}, \quad (33)$$

$$F_{(b)y} = \frac{G\lambda_0 y\left[(z-a)\,\mathcal{R}_1 - (z+a)\,\mathcal{R}_2\right]}{(x^2+y^2+b^2)\,\mathcal{R}_1\mathcal{R}_2} - 3\varepsilon\frac{G\lambda_0 z}{a^2}\ln\left(\frac{z-a+\mathcal{R}_2}{z+a+\mathcal{R}_1}\right)$$

$$+\varepsilon\frac{G\lambda_0}{a^2\,(x^2+y^2+b^2)^2\,\mathcal{R}_1^3\mathcal{R}_2^3}\left\{\mathcal{R}_1^3\left[\left(x^2+y^2+b^2+z^2\right)^2\right.\right.$$

$$\times\left[2\left(x^2+y^2+b^2\right)\left(x^2+2y^2+b^2\right) + z^2\left(y^2-x^2-b^2\right)\right]$$

$$-az^3\left(y^2-x^2-b^2\right)\left(a^2-3az+3z^2\right) + a^4\left(x^2+y^2+b^2\right)^2$$

$$-3a\left(x^2+y^2+b^2\right)^2\left[z\left(3x^2+5y^2+3b^2\right) - a\left(x^2+2y^2+b^2\right)\right]$$

$$-az\left(x^2+y^2+b^2\right)\left[-3az\left(4x^2+7y^2+4b^2\right) + 6z^2\left(x^2+3y^2+b^2\right)\right.$$

$$\left.\left.+a^2\left(7x^2+10y^2+7b^2\right)\right]\right] - \mathcal{R}_2^3\left[\left(x^2+y^2+b^2+z^2\right)^2\right.$$

$$\times\left[2\left(x^2+y^2+b^2\right)\left(x^2+2y^2+b^2\right) + z^2\left(y^2-x^2-b^2\right)\right]$$

$$+az^3\left(y^2-x^2-b^2\right)\left(a^2+3az+3z^2\right) + a^4\left(x^2+y^2+b^2\right)^2$$

$$+3a\left(x^2+y^2+b^2\right)^2\left[z\left(3x^2+5y^2+3b^2\right) + a\left(x^2+2y^2+b^2\right)\right]$$

$$+az\left(x^2+y^2+b^2\right)\left[3az\left(4x^2+7y^2+4b^2\right) + 6z^2\left(x^2+3y^2+b^2\right)\right.$$

$$\left.\left.+a^2\left(7x^2+10y^2+7b^2\right)\right]\right]\right\}, \quad (34)$$

$$F_{(b)z} = \frac{G\lambda_0\left(\mathcal{R}_2-\mathcal{R}_1\right)}{\mathcal{R}_1\mathcal{R}_2} - 3\varepsilon\frac{G\lambda_0 y}{a^2}\ln\left(\frac{z-a+\mathcal{R}_2}{z+a+\mathcal{R}_1}\right)$$

$$-\varepsilon\frac{G\lambda_0 y}{a^2\,(x^2+y^2+b^2)\,\mathcal{R}_1^3\mathcal{R}_2^3}\left\{\mathcal{R}_1^3\left[3z\left(x^2+y^2+b^2+z^2\right)^2\right.\right.$$

$$-a\left(x^2+y^2+b^2\right)\left(6z^2+3az-4a^2\right) + 3a\left(x^2+y^2+b^2\right)^2$$

$$\left.-3az^2\left(3z^2-3az+a^2\right)\right] - \mathcal{R}_2^3\left[3z\left(x^2+y^2+b^2+z^2\right)^2\right.$$

$$+a\left(x^2+y^2+b^2\right)\left(6z^2-3az-4a^2\right) - 3a\left(x^2+y^2+b^2\right)^2$$

$$\left.\left.+3az^2\left(3z^2+3az+a^2\right)\right]\right\}. \quad (35)$$

23

In all equations, we have $\mathcal{R}_1 = \sqrt{x^2 + y^2 + b^2 + (z+a)^2}$, and $\mathcal{R}_2 = \sqrt{x^2 + y^2 + b^2 + (z-a)^2}$.

B Components of forces for non-axisymmetric thin distributions of matter

The components of the force $\mathbf{F}_{(a)} = -\nabla\Phi_{(a)}$, on the plane $z = 0$, after applying the transformations $z \to x$ and $x \to z$, then $z \to c + |z|$, on the potential (16), read

$$
\begin{aligned}
\mathrm{F}_{(a)x} = {} & \frac{G\lambda_0\,(\mathrm{R}_2 - \mathrm{R}_1)}{\mathrm{R}_1\mathrm{R}_2} + \varepsilon \frac{G\lambda_0 y}{a\,(y^2 + c^2)\,\mathrm{R}_1^3\mathrm{R}_2^3} \left\{ \mathrm{R}_2^3 \left[2\left(x^2 + y^2 + c^2\right)^2 \right.\right. \\
& + 3a\left(y^2 + c^2\right)(a + 2x) + 2ax\left(a^2 + 3ax + 3x^2\right) \Big] - \mathrm{R}_1^3 \Big[2\left(x^2 + y^2 + c^2\right)^2 \\
& \left.\left. + 3a\left(y^2 + c^2\right)(a - 2x) - 2ax\left(a^2 - 3ax + 3x^2\right) \right] \right\},
\end{aligned}
\tag{36}
$$

$$
\begin{aligned}
\mathrm{F}_{(a)y} = {} & \frac{G\lambda_0 y\,[(x-a)\,\mathrm{R}_1 - (x+a)\,\mathrm{R}_2]}{(y^2 + c^2)\,\mathrm{R}_1\mathrm{R}_2} - \varepsilon\frac{G\lambda_0}{a}\ln\left(\frac{x - a + \mathrm{R}_2}{x + a + \mathrm{R}_1}\right) \\
& + \varepsilon\frac{G\lambda_0}{a\,(y^2 + c^2)^2\,\mathrm{R}_1^3\mathrm{R}_2^3} \left\{ \mathrm{R}_1^3\left[x\left(x^2 + y^2 + c^2\right)^2\left(y^2 - c^2\right) \right.\right. \\
& \qquad\qquad - a\left(x^2 + y^2 + c^2\right)\left[3x^2\left(y^2 - c^2\right) + \left(y^2 + c^2\right)^2 \right] \\
& \left. - a^2\left(y^2 + c^2\right)\left[a\left(2y^2 + c^2\right) - x\left(4y^2 + c^2\right) \right] - a^2x^2\left(y^2 - c^2\right)(a - 3x) \right] \\
& - \mathrm{R}_2^3\left[x\left(x^2 + y^2 + c^2\right)^2\left(y^2 - c^2\right) + a\left(x^2 + y^2 + c^2\right)\left[3x^2\left(y^2 - c^2\right) + \left(y^2 + c^2\right)^2 \right] \right. \\
& \left.\left. + a^2\left(y^2 + c^2\right)\left[a\left(2y^2 + c^2\right) + x\left(4y^2 + c^2\right) \right] + a^2x^2\left(y^2 - c^2\right)(a + 3x) \right] \right\}.
\end{aligned}
\tag{37}
$$

The components of the force $\mathbf{F}_{(b)} = -\nabla\Phi_{(b)}$, on the plane $z = 0$, after applying the transformations $z \to x$ and $x \to z$, then $z \to c + |z|$, on the

potential (17), read

$$
\begin{aligned}
F_{(b)x} ={}& \frac{G\lambda_0\left(R_2 - R_1\right)}{R_1 R_2} - 3\varepsilon\frac{G\lambda_0 y}{a^2}\ln\left(\frac{x - a + R_2}{x + a + R_1}\right) - \varepsilon\frac{G\lambda_0 y}{a^2\left(y^2 + c^2\right)R_1^3 R_2^3} \\
&\times\left\{R_1^3\left[3x\left(x^2 + y^2 + c^2\right)^2 - a\left(y^2 + c^2\right)\left(6x^2 + 3ax - 4a^2\right) + 3a\left(y^2 + c^2\right)^2\right.\right. \\
&\left.- 3ax^2\left(3x^2 - 3ax + a^2\right)\right] - R_2^3\left[3x\left(x^2 + y^2 + c^2\right)^2\right. \\
&\left.\left.+ a\left(y^2 + c^2\right)\left(6x^2 - 3ax - 4a^2\right) - 3a\left(y^2 + c^2\right)^2 + 3ax^2\left(3x^2 + 3ax + a^2\right)\right]\right\},
\end{aligned}
$$
(38)

$$
\begin{aligned}
F_{(b)y} ={}& \frac{G\lambda_0 y\left[\left(x - a\right)R_1 - \left(x + a\right)R_2\right]}{\left(y^2 + c^2\right)R_1 R_2} - 3\varepsilon\frac{G\lambda_0 x}{a^2}\ln\left(\frac{x - a + R_2}{x + a + R_1}\right) \\
&+ \varepsilon\frac{G\lambda_0}{a^2\left(y^2 + c^2\right)^2 R_1^3 R_2^3}\left\{R_1^3\left[\left(x^2 + y^2 + c^2\right)^2\left[2\left(y^2 + c^2\right)\left(2y^2 + c^2\right)\right.\right.\right. \\
&\left.+ x^2\left(y^2 - c^2\right)\right] - ax^3\left(y^2 - c^2\right)\left(a^2 - 3ax + 3x^2\right) + a^4\left(y^2 + c^2\right)^2 \\
&- 3a\left(y^2 + c^2\right)^2\left[x\left(5y^2 + 3c^2\right) - a\left(2y^2 + c^2\right)\right] \\
&\left.- ax\left(y^2 + c^2\right)\left[-3ax\left(7y^2 + 4c^2\right) + 6x^2\left(3y^2 + c^2\right) + a^2\left(10y^2 + 7c^2\right)\right]\right] \\
&- R_2^3\left[\left(x^2 + y^2 + c^2\right)^2\left[2\left(y^2 + c^2\right)\left(2y^2 + c^2\right) + x^2\left(y^2 - c^2\right)\right]\right. \\
&+ ax^3\left(y^2 - c^2\right)\left(a^2 + 3ax + 3x^2\right) + a^4\left(y^2 + c^2\right)^2 \\
&+ 3a\left(y^2 + c^2\right)^2\left[x\left(5y^2 + 3c^2\right) + a\left(2y^2 + c^2\right)\right] \\
&\left.\left.+ ax\left(y^2 + c^2\right)\left[3ax\left(7y^2 + 4c^2\right) + 6x^2\left(3y^2 + c^2\right) + a^2\left(10y^2 + 7c^2\right)\right]\right]\right\}.
\end{aligned}
$$
(39)

In all equations, we have $R_1 = \sqrt{y^2 + c^2 + \left(x + a\right)^2}$ and
$R_2 = \sqrt{y^2 + c^2 + \left(x - a\right)^2}$.